

Electronic Supplementary Information

MOF-derived Ordered Porous Nitrogen-doped Carbon Integrated with Pt₃Co Alloy Catalyst for Efficient Oxygen Reduction Reaction

Rui Wu, Jiayu Zuo, Lei Zhao, Zhaozhao Zhu, Qiyu Li, Xiaobin Niu *, and Jun Song Chen*

School of Materials and Energy, University of Electronic Science and Technology of China, Chengdu 611731, China. *Corresponding author E-mail: xbniu@uestc.edu.cn (X. Niu); jschen@uestc.edu.cn (J. S. Chen)

1. Experimental Section

1.1. Materials

Ammonia ($\text{NH}_3 \cdot \text{H}_2\text{O}$, 25%), zinc nitrate hexahydrate ($\text{Zn}(\text{NO}_3)_2 \cdot 6\text{H}_2\text{O}$, 98%), hydrofluoric acid (HF, 40%), and perchloric acid (HClO_4 , AR) were purchased from Sinopharm Chemical Reagent Co., Ltd. 2-Methylimidazole (2-MeIm, 98%) and cobalt nitrate hexahydrate ($\text{Co}(\text{NO}_3)_2 \cdot 6\text{H}_2\text{O}$, AR) were provided by Aladdin Biochemical Technology Co., Ltd. Methanol (99.5%), anhydrous ethanol (99.7%), and hydrochloric acid (HCl, AR) were acquired from Chengdu Kelong Chemical Co., Ltd. Tetraethyl orthosilicate (TEOS, 98%) was supplied by Shanghai Meryer Chemical Technology Co., Ltd. Chloroplatinic acid hexahydrate ($\text{H}_2\text{PtCl}_6 \cdot 6\text{H}_2\text{O}$, 38%) were sourced from Sino-Platinum Metals Co., Ltd.

1.2. Synthesis of the $\text{Pt}_3\text{Co-NC-800}$ catalyst

Silica spheres were synthesized using the Stöber method.¹ Typically, 15 mL of TEOS was mixed with 225 mL of ethanol, 30 mL of deionized water, and an ammonia solution (28-30 wt.%) in a glass bottle, followed by stirring for 2 hours. Subsequent centrifugation and drying at 60°C for 12 hours yielded the silica spheres.

A 500 mg of silica spheres were combined with 747.2 mg of $\text{Zn}(\text{NO}_3)_2 \cdot 6\text{H}_2\text{O}$ and 980 mg of 2-MeIm, dissolved in 40 mL of methanol, and stirred for 2 hours. Subsequently, the mixture was incubated at 60°C for 24 hours to facilitate the growth of a zeolitic imidazolate framework (ZIF-8) within the silica matrix, resulting in a $\text{SiO}_2@\text{ZIF-8}$ composite. This composite was annealed at 900°C under an argon atmosphere for 2 hours, followed by leaching with HF to yield a porous nitrogen-doped carbon (NC) support. Next, 120 mg of the NC support was dispersed in 30 mL of H_2PtCl_6 solution ($0.5 \text{ mg}_{\text{Pt}} \text{ mL}^{-1}$). Subsequently, 1550 μL of $\text{Co}(\text{NO}_3)_2$ (0.1 mol L^{-1}) solution was added dropwise, and the mixture was stirred overnight. This preparation was dried and subjected to pyrolysis at 800°C for 2 hours under an Ar/ H_2 (5%) atmosphere to synthesize the $\text{Pt}_3\text{Co-NC-800}$ catalyst. The catalyst was then washed with 0.1 M HCl and dried.

For comparison, additional $\text{Pt}_3\text{Co-NC}$ catalysts were synthesized by a similar procedure by modifying pyrolysis temperatures, durations, and Pt contents while maintaining a Pt:Co molar ratio of 1:2.

1.3. Characterization

The morphological features of the catalysts were characterized using scanning electron microscopy (SEM, Phenom XL) and transmission electron microscopy (TEM, JEM2010F). The crystalline phase and structural composition of the catalyst materials were investigated by X-ray diffractometer (XRD, PANalytical Aries, Cu-

$K\alpha$, $\lambda = 0.1540$ nm). Nitrogen adsorption-desorption isotherms were collected using a KuBo-X1000 instrument. X-ray photoelectron spectroscopy (XPS) measurements were conducted using a Thermo Fisher Scientific, Escalab 250Xi with Al $K\alpha$ radiation. The Pt content was quantified using inductively coupled plasma mass spectrometry (ICP-MS, Agilent 720ES).

1.4. Electrochemical Measurements

1.4.1 RDE measurements.

A homogeneous catalyst ink was prepared by ultrasonically dispersing 2.0 mg of the as-prepared catalyst in a mixture of isopropanol (790 μL) and Nafion (10 μL , 5 wt%). The ink was then meticulously dropwise applied onto a glassy-carbon rotating disk electrode (RDE), achieving a catalyst loading of 20.4 $\mu\text{g}_{\text{Pt}} \text{cm}^{-2}$ for each catalyst type, including Pt/C.

Cyclic Voltammetry (CV) was conducted under N_2 -saturated conditions in 0.1 M HClO_4 at a scan rate of 50 mV s^{-1} . Linear Sweep Voltammetry (LSV) measurements were performed in O_2 -saturated 0.1 M HClO_4 , using a rotation speed of 1600 rpm and a sweep rate of 10 mV s^{-1} . An accelerated durability test (ADT) was performed by repetitive potential cycles between 0.6 and 1.0 V vs. RHE at 100 mV s^{-1} for 30,000 cycles in an O_2 -saturated electrolyte.

The Electrochemical Active Surface Area (ECSA) was determined using a CO stripping test. This test involved bubbling CO into the 0.1 M HClO_4 electrolyte and maintaining the potential at 0.05 V for 30 minutes, followed by purging the electrolyte with N_2 for an additional 30 minutes. Subsequently, the cyclic voltammogram was recorded by scanning the potential from 0.05 V to 1.05 V at a scan rate of 50 mV s^{-1} . The ECSA was calculated from the formula: $\text{ECSA} = (S_{\text{CO}}/V)/(0.42 \times L_{\text{Pt}})$, where S_{CO} is the integration area of CO desorption, V is the sweep speed, and L_{Pt} is the Pt loading.

1.4.2 MEA measurements.

The catalyst ink comprises a catalyst, ionomer, and ink dispersion solvent. Nafion is used as the ionomer, while a mixture of volatile isopropanol and ultrapure water is selected as the ink dispersion solvent. The ionomer content is controlled based on the amount of carbon black in the catalyst support, with an I/C ratio of 0.6. The ratio of isopropanol to ultrapure water is 12:1. The membrane electrode was prepared using a spray coating method. The prepared ink was ultrasonically dispersed to ensure uniformity. A spray gun connected to high-pressure gas was used, with adjustments to the liquid and gas flow rates to ensure rapid mist-like

evaporation during spraying. A vacuum pump was employed to assist in catalyst ink adsorption on both sides of the proton exchange membrane. The proton exchange membrane was cut to 2.5 cm×2.5 cm. The catalyst-coated membrane was prepared with an effective active area of 5.0 cm², where the catalyst ink was uniformly adsorbed on both sides of the proton exchange membrane. Pt₃Co-NC-800 and commercial Pt/C (40 wt%) were used as cathode and anode catalysts, respectively. The electrode area for the MEA test was 5.0 cm². The catalyst loadings were 0.06 mg_{Pt} cm⁻² for the cathode and 0.1 mg_{Pt} cm⁻² for the anode. The carbon paper size matched the effective active area of the proton exchange membrane, measuring 5.0 cm². A hot-pressing method was applied to tightly bond with the proton exchange membrane, which carried the catalyst ink, to the carbon paper, forming a complete membrane electrode assembly (MEA). Assemble the fuel cell by sequentially placing the metal end plates, current collector plates, flow field plates, sealing gaskets, and MEA. The assembly torque is set to 4.5 N·m, and the effective active area of the membrane electrode is fixed at 5 cm².

For H₂-O₂ single-cell tests, MEA tests were performed using a fuel cell workstation (Mini 150, Hephass Energy Co.) at 80 °C with a backpressure of 250 kPa for both the anode and the cathode. H₂ (anode) and O₂ (cathode) with 100% relative humidity were supplied at flow rates of 500 and 1000 sccm, respectively.

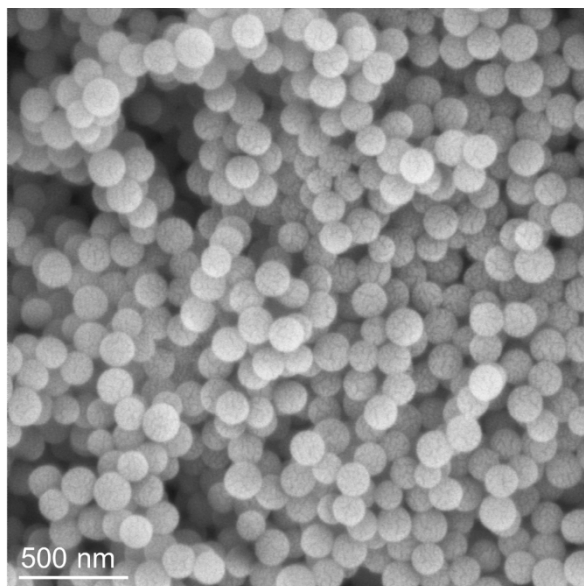


Fig. S1 SEM image of SiO₂ nanospheres.

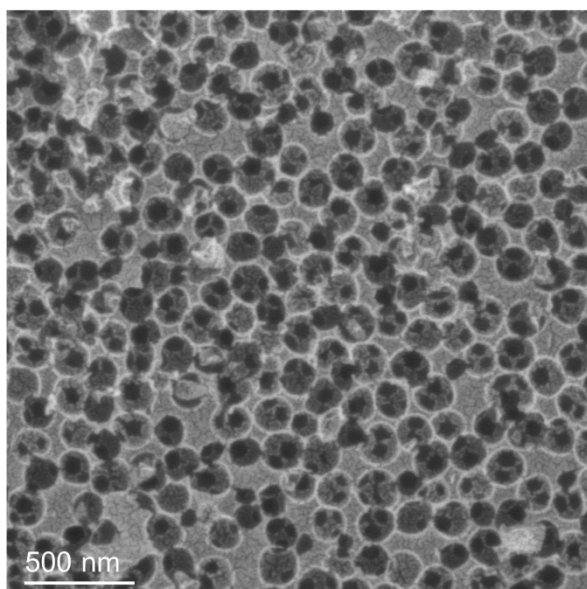


Fig. S2 SEM image of NC.

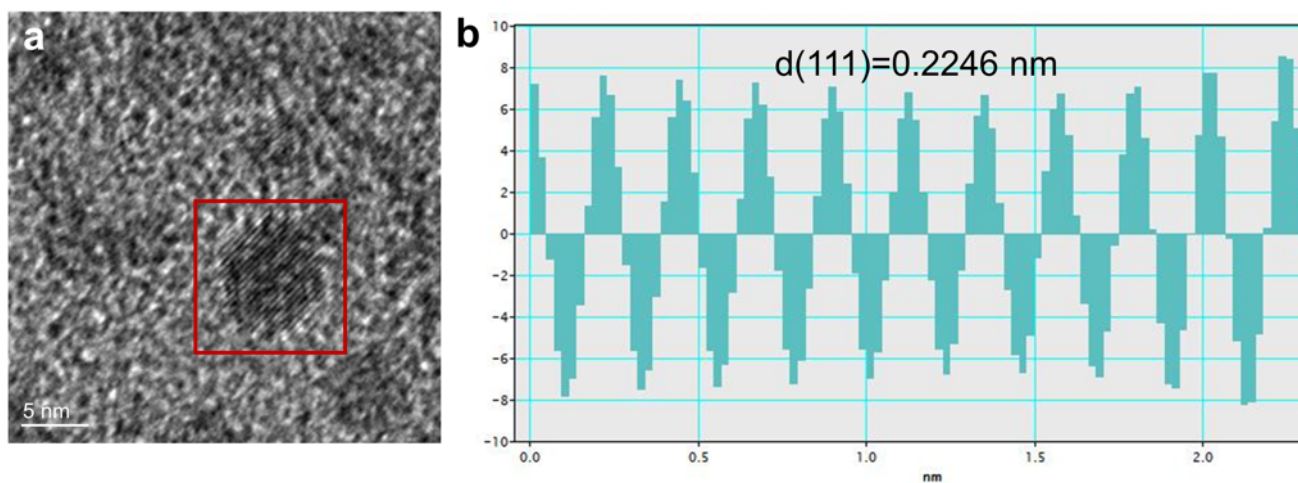


Fig. S3 HR-TEM image of (a) Pt₃Co-NC-800 and (b) corresponding lattice spacing analysis of IFFT pattern.

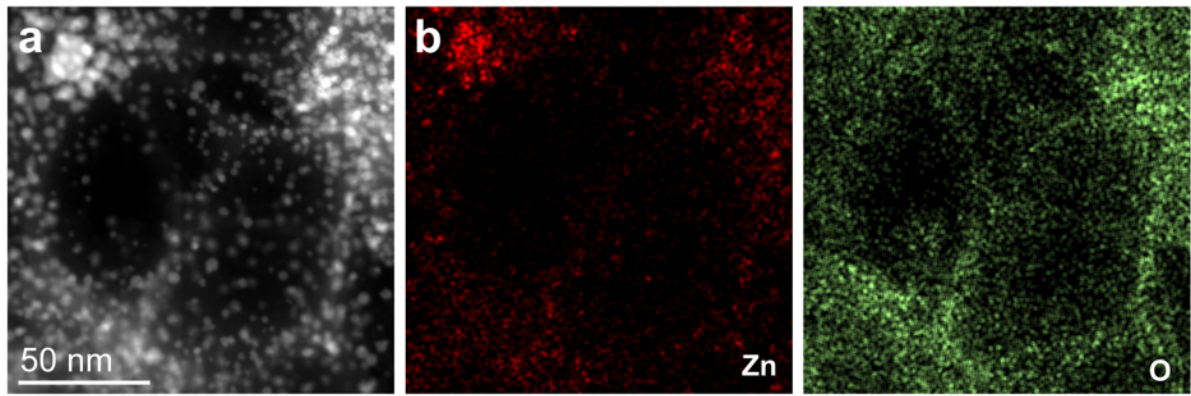


Fig. S4 (a, b) The Zn and O elemental mappings in Pt₃Co-NC-800.

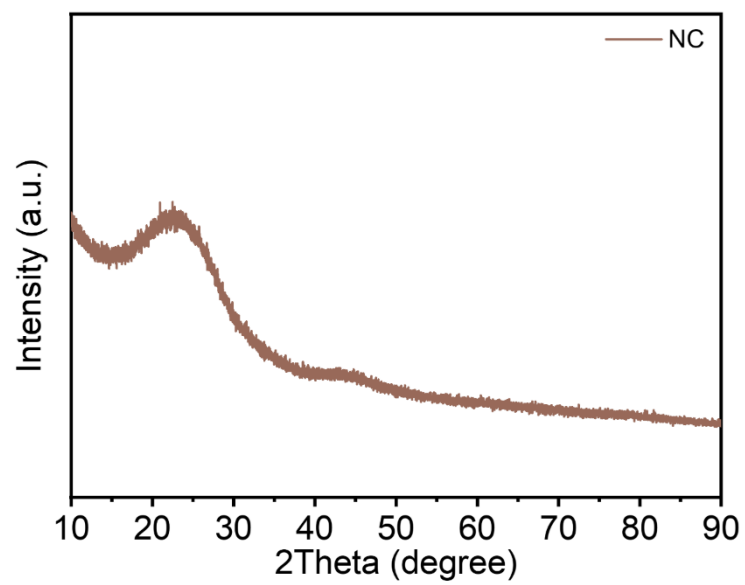


Fig. S5 XRD spectrum of NC.

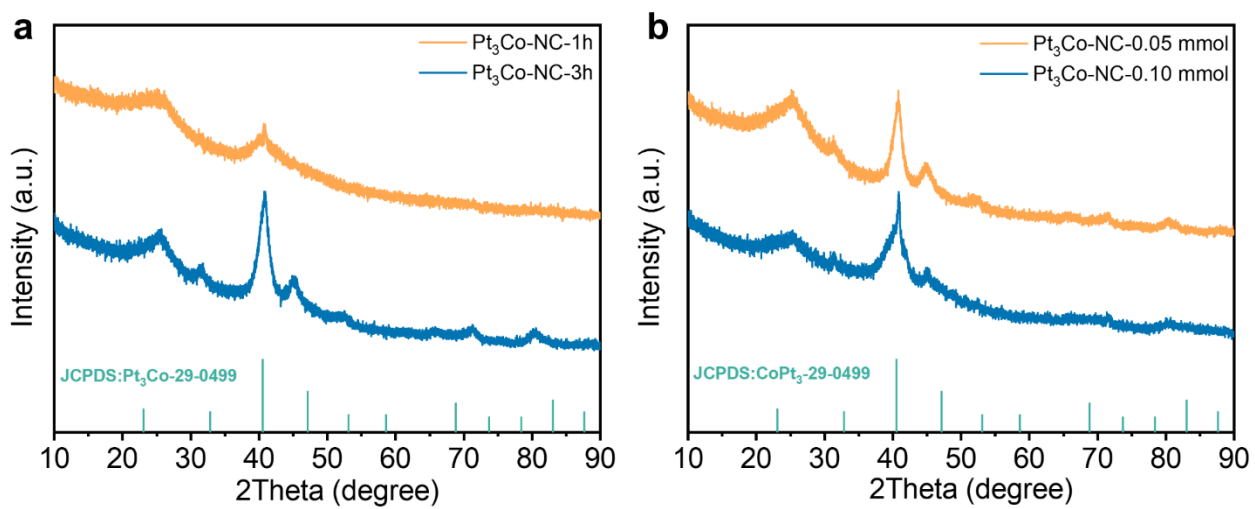


Fig. S6 XRD spectra of (a) different Pt₃Co-NC products synthesized at 800 °C with different durations and (b) different Pt₃Co-NC catalysts synthesized with different Pt contents.

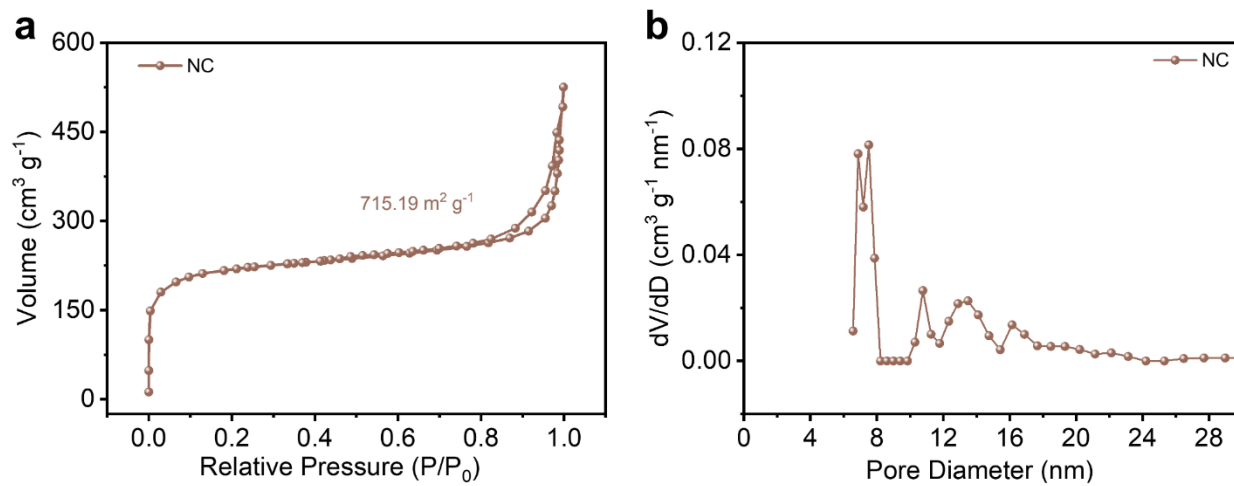


Fig. S7 (a) Nitrogen adsorption/desorption isotherm and (b) corresponding the pore size distribution of NC.

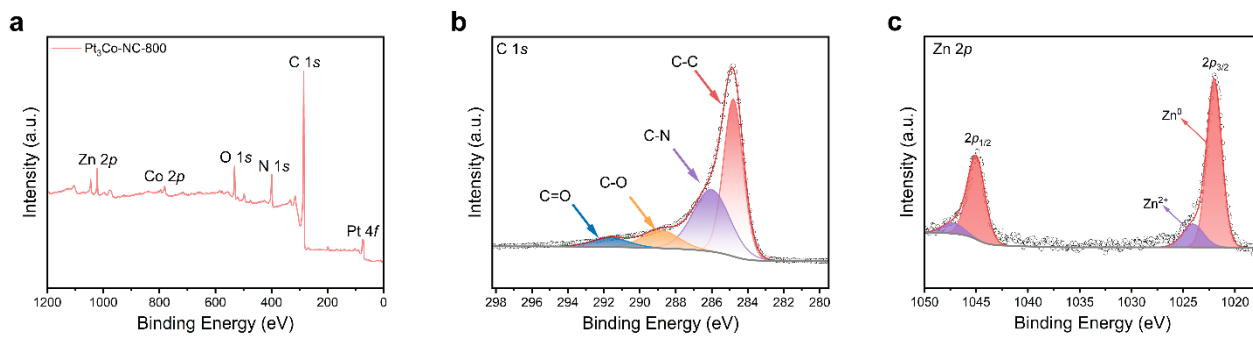


Fig. S8 XPS survey spectra of (a) Pt₃Co-NC-800 and corresponding high-resolution; (b) C 1s spectrum and (c) Zn 2p spectrum.

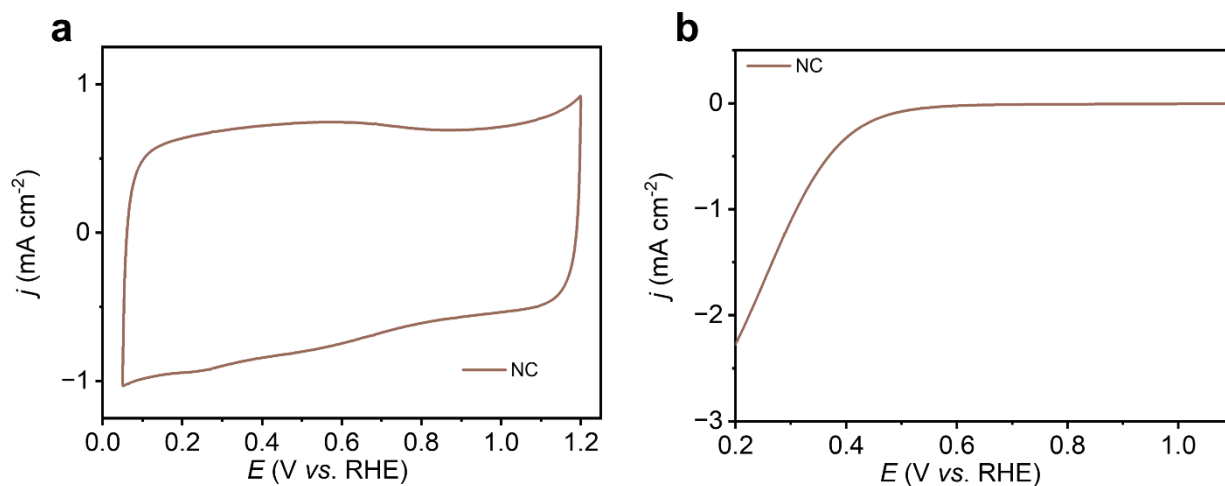


Fig. S9 The NC catalyst. (a) CV curve in 0.1 M N₂-saturated HClO₄ electrolyte. (b) LSV curve in 0.1 M O₂-saturated HClO₄ electrolyte at 1,600 rpm with a scan rate of 10 mV s⁻¹.

As shown in Fig. S9, the NC support displayed limited catalytic activity for the ORR, indicating that the Zn species in the NC support have a negligible effect on the activity.

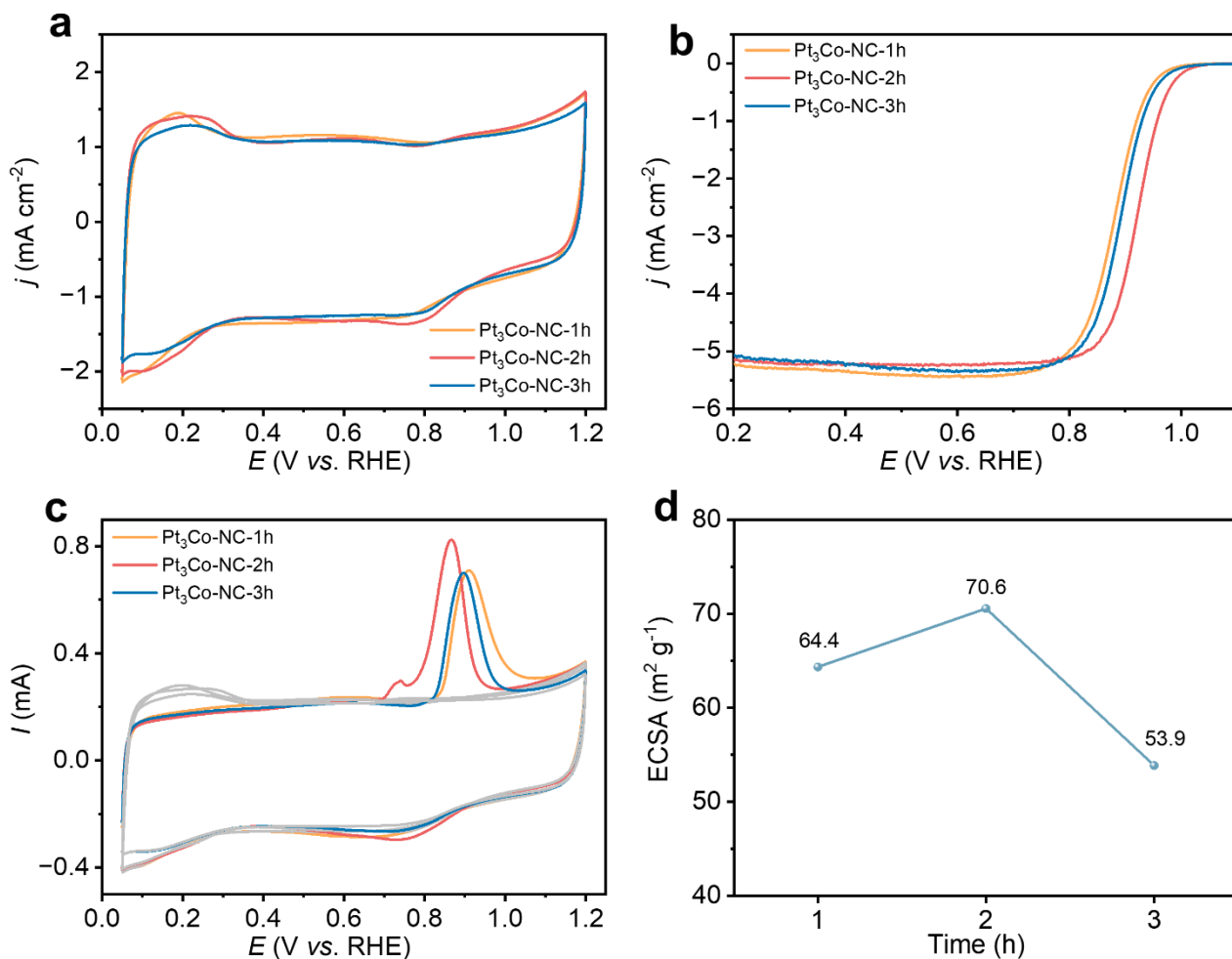


Fig. S10 ORR catalytic activities for different Pt₃Co-NC products obtained at 800 °C over different durations. (a) CV curves of in 0.1 M HClO₄ saturated with N₂ at a scan rate of 50 mV s⁻¹. (b) LSV curves in 0.1 M HClO₄ saturated with O₂ at 1,600 rpm and a scan rate of 10 mV s⁻¹. (c) CO stripping voltammograms. (d) ECSA comparison.

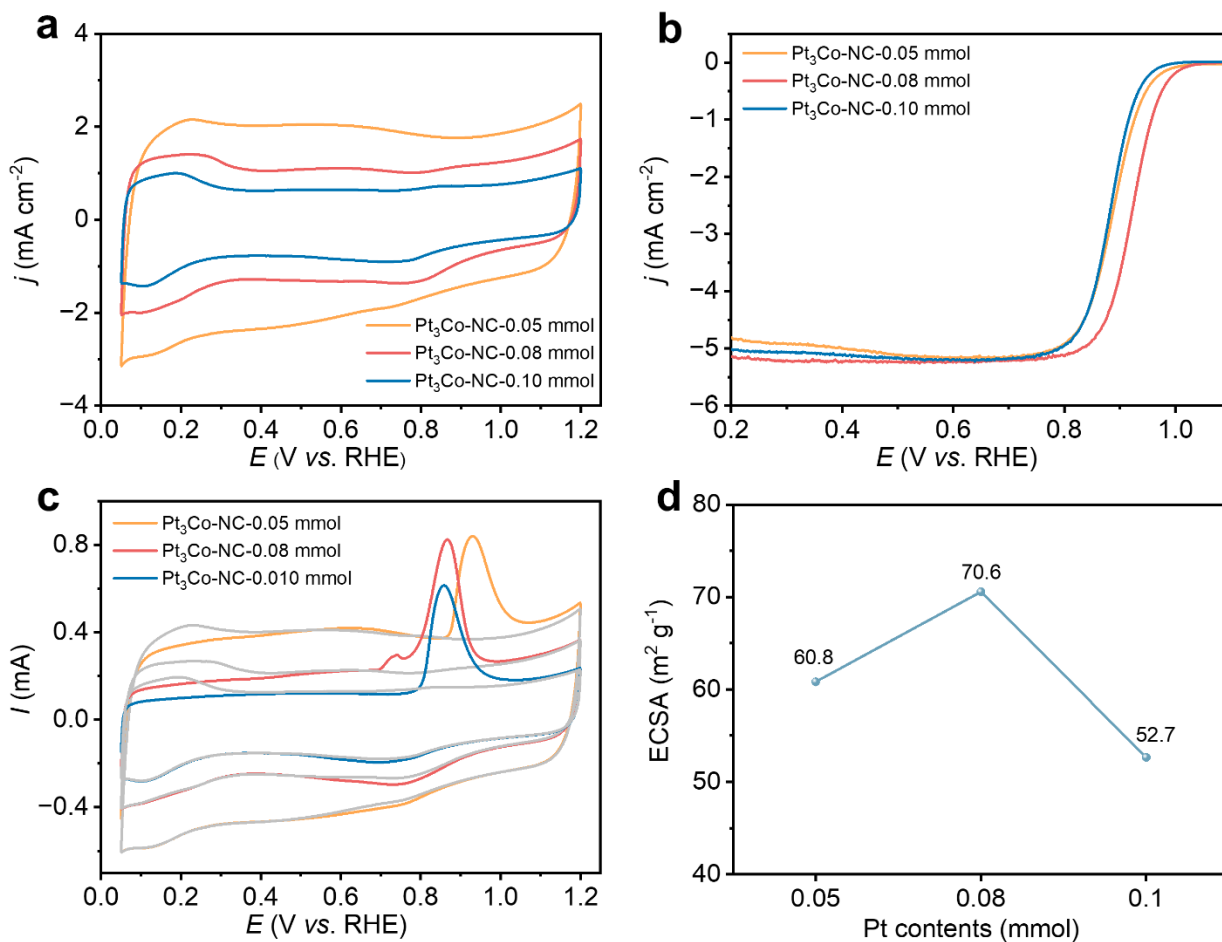


Fig. S11 ORR catalytic activities for different Pt₃Co-NC products synthesized with different Pt contents. (a) CV curves of in 0.1 M HClO₄ saturated with N₂ at a scan rate of 50 mV s⁻¹. (b) LSV curves in 0.1 M HClO₄ saturated with O₂ at 1,600 rpm and a scan rate of 10 mV s⁻¹. (c) CO stripping voltammograms. (d) ECSA comparison.

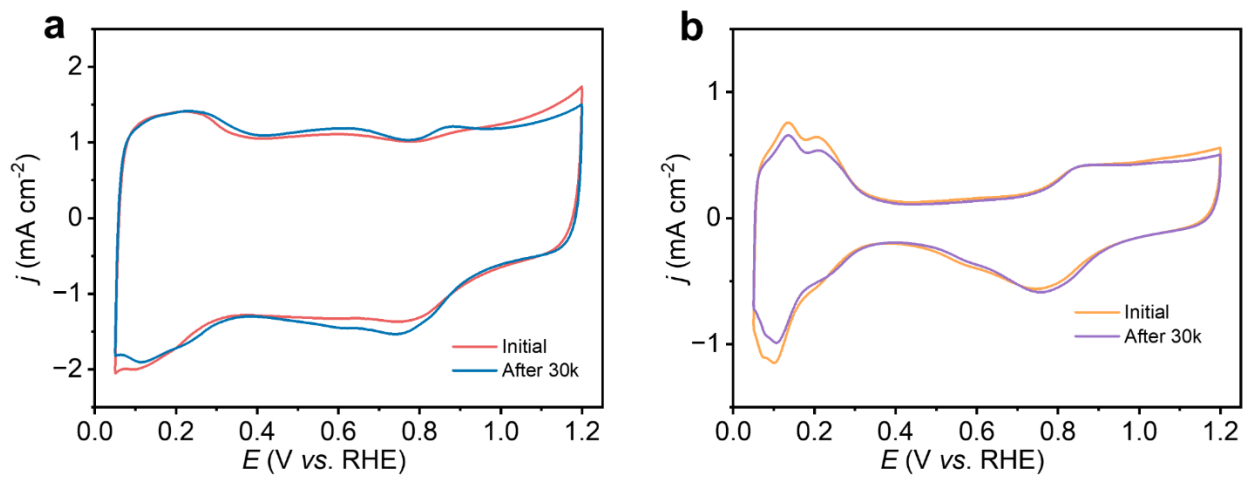


Fig. S12 CV curves of (a) Pt₃Co-NC-800 and (b) Pt/C before and after 30,000 cycles ADT.

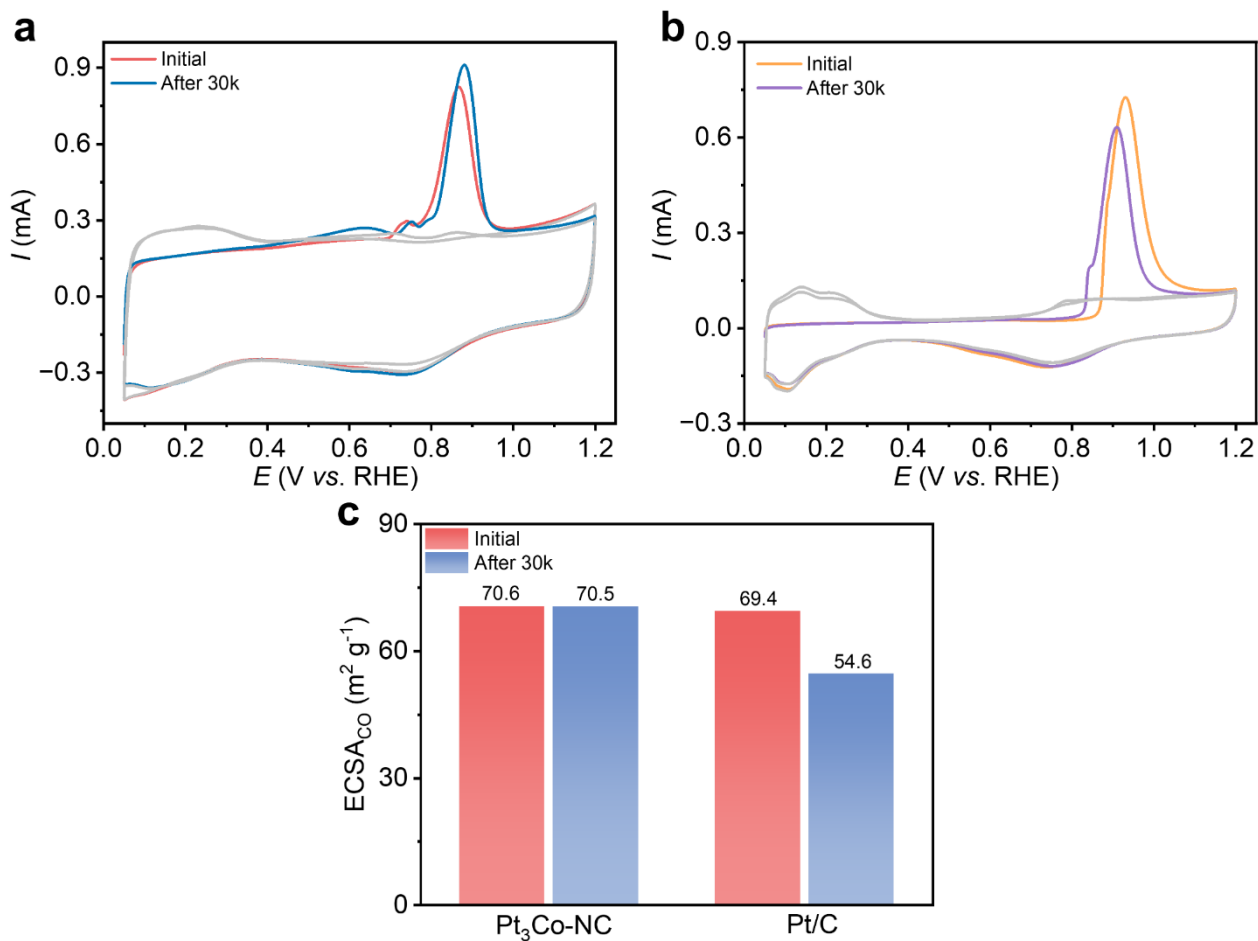


Fig. S13 CO stripping voltammograms of (a) Pt₃Co-NC-800 and (b) Pt/C before and after 30,000 cycles, and (c) corresponding ECSA comparison.

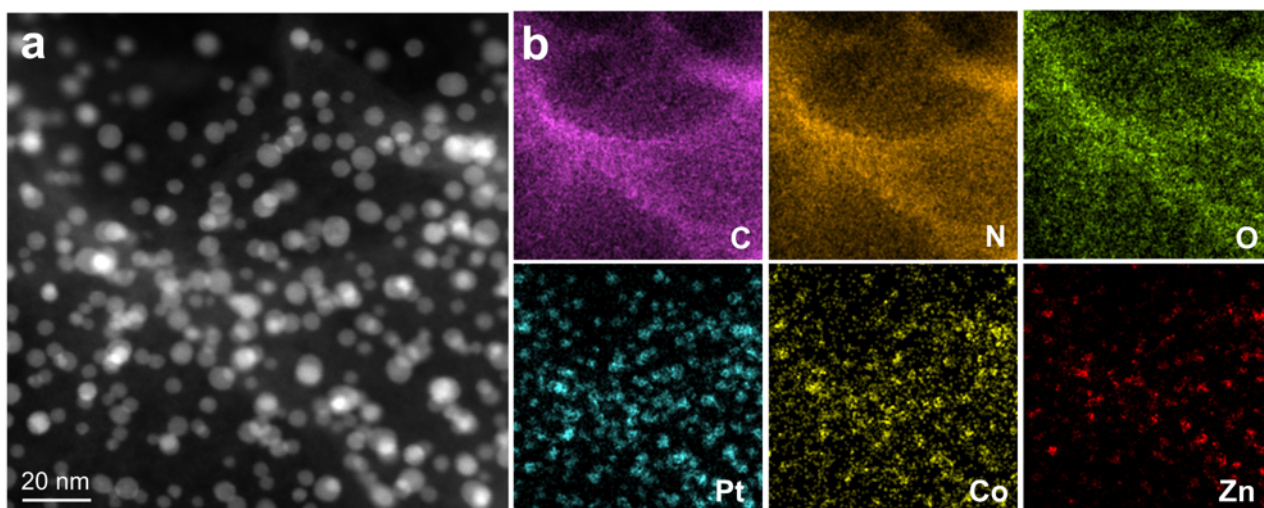


Fig. S14 STEM image of (a) Pt₃Co-NC-800 and (b) EDS elemental mappings after 30,000 potential cycles.

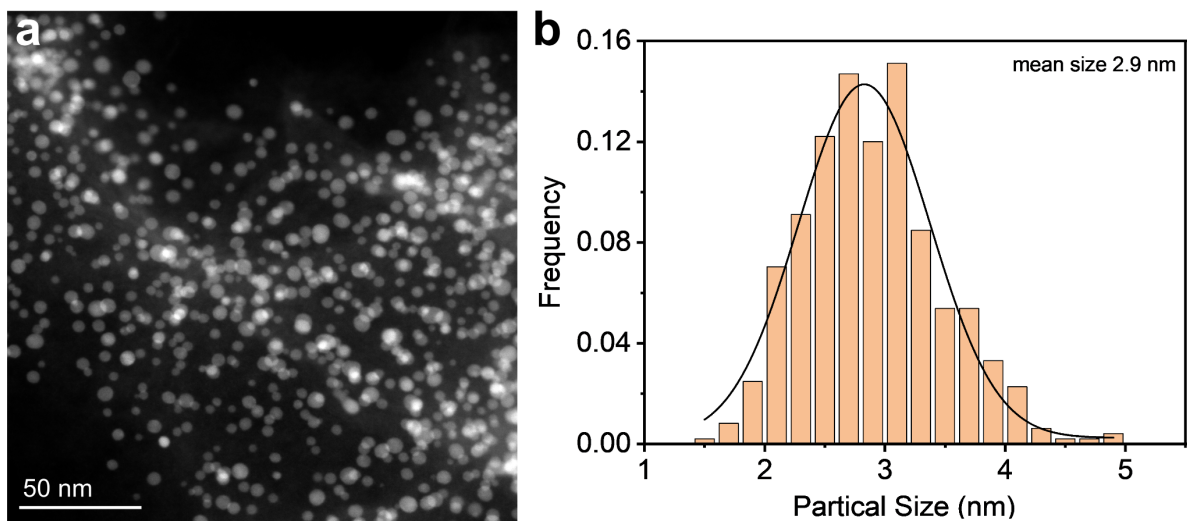


Fig. S15 STEM image of (a) Pt₃Co-NC-800 and (b) corresponding size distribution histogram after 30,000 potential cycles.

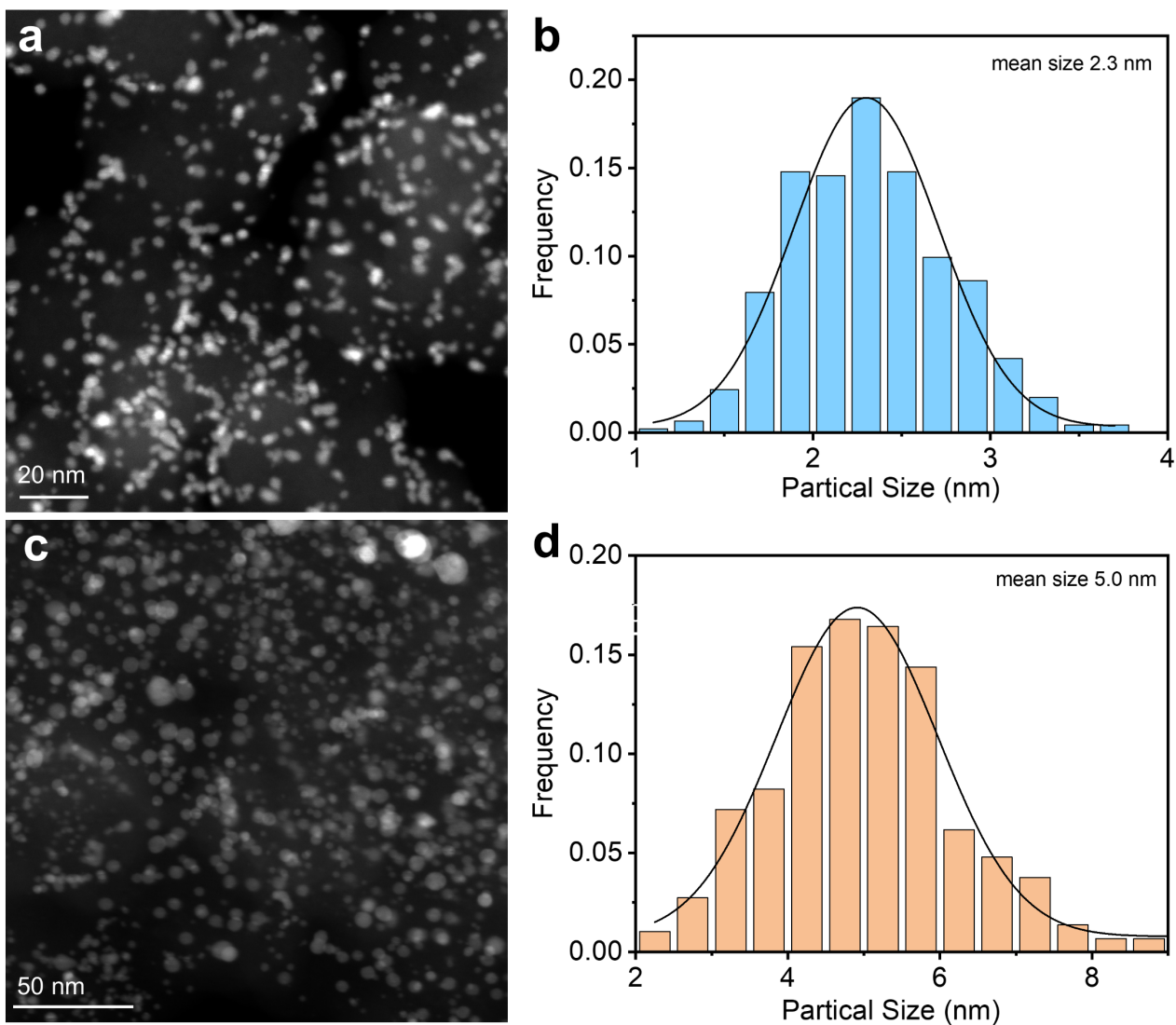


Fig. S16 STEM images and corresponding Pt nanoparticles size distributions of (a, b) fresh Pt/C catalyst and (c, d) aged Pt/C catalyst after 30,000 cycles.

Table S1 Elemental composition analysis of the as-synthesized catalysts determined by ICP-MS.

Catalyst	Pt (wt%)	Co (wt%)
Pt ₃ Co-NC-750	14.6	4.0
Pt ₃ Co-NC-800	15.0	4.1
Pt ₃ Co-NC-850	18.9	4.4
Pt ₃ Co-NC-900	20.4	4.8

Table S2 Comparison of the ORR performance of different Pt₃Co-NC products.

Catalyst	Pt₃Co-NC- 1 h	Pt₃Co-NC- 3 h	Pt₃Co-NC- 0.05 mmol	Pt₃Co-NC- 0.10 mmol	Pt₃Co-NC- 800
Pt loading (wt%)	12.0%	11.6%	7.6%	16.2%	15.0%
E _{1/2} (V vs. RHE)	0.881	0.893	0.890	0.883	0.922
J _d (mA cm ⁻²)	5.34	5.20	4.98	5.09	5.22
ECSA _{Co} (m ² g ⁻¹)	64.4	53.9	60.8	52.7	70.6

Table S3 Comparison of durability tests of recently reported Pt electrocatalysts.

Catalyst	$E_{1/2}$ (V)	MA ($\text{A mg}_{\text{Pt}}^{-1}$)	Loss of $E_{1/2}$ (mV) after ADTs	Loss of MA after ADTs (%)	References
Pt₃Co-NC-800	0.922	0.62	1 (30k)	1.8 (30k)	This Work
PtCo/P _{2.73} O _x -KB	0.928	1.11	13 (50k)	34 (50k)	2
Pt ₃ FeCo NSs/C	0.963	4.66	/	20.8 (30k)	3
PtCo@Pt/C-6	/	0.996	7 (30k)	20 (30k)	4
Pt ₈₃ Ni ₁₇ BNCs AG/C	0.940	1.95	6.1 (20k)	17.4 (20k)	5
L1 ₀ -PtCo _{0.50} Fe _{0.50}	0.945	0.93	11 (30k)	24.7 (30k)	6
L1 ₂ -Pt ₃ Co	0.917	0.31	9 (5k)	6.2 (5k)	7
PtCo-PtSn/C	0.930	1.16	20 (30k)	27.4 (30k)	8
Pt ₃ Ni _{aer} -C=C	0.931	0.57	12 (5k)	/	9
Pt/HFe _{SA} -HCS	0.910	0.98	11 (20k)	3.0 (30k)	10
Pt@Fe-NC	0.936	1.34	12 (20k)	14.0 (20k)	11

References

1. W. Stöber, A. Fink and E. Bohn, *J. Colloid Interface Sci.*, 1968, **26**, 62-69.
2. S.-N. Hu, W.-C. Xu, N. Tian, S.-M. Chen, M.-Y. Li, J.-F. Shen, J.-X. Lin, S.-L. Guo, X.-Y. Huang, Z.-Y. Zhou and S.-G. Sun, *Energy Environ. Sci.*, 2024, **17**, 3099-3111.
3. L. Bu, J. Liang, F. Ning, J. Huang, B. Huang, M. Sun, C. Zhan, Y. Ma, X. Zhou, Q. Li and X. Huang, *Adv. Mater.*, 2023, **35**, 2208672.
4. Y. Jiang, Q. Zhang, J. Qian, Y. Wang, Y. Mu, Z. Zhang, Z. Li, T. Zhao, B. Liu and L. Zeng, *ACS Catal.*, 2024, **14**, 6992-7000.
5. Y. Zheng, A. S. Petersen, H. Wan, R. Hübner, J. Zhang, J. Wang, H. Qi, Y. Ye, C. Liang, J. Yang, Z. Cui, Y. Meng, Z. Zheng, J. Rossmeisl and W. Liu, *Adv. Energy Mater.*, 2023, **13**, 2204257.
6. Y. Hu, M. Lu, G. Zhang, X. Zhao, Y. Liu, X. Yang, X. Yu, X. Zhang, Z. Lu and L. Li, *Appl. Catal. B-Environ.*, 2025, **360**, 124556.
7. Y. Su, Z. Wang, R. Gao, Q. Wu, J. Zhao, G. Zhu, Q. Li, H. Xu, Y. Pan, K. Gu, C. Biz, M. Fianchini and J. Gracia, *Adv. Funct. Mater.*, 2024, **34**, 2311618.
8. J. Chen, G. Qian, B. Chu, Z. Jiang, K. Tan, L. Luo, B. Li and S. Yin, *Small*, 2022, **18**, 2106773.
9. H. Yuan, W. Gao, X. Wan, J. Ye and D. Wen, *J. Energy Chem.*, 2024, **89**, 557-564.
10. W. Yan, Q. Xing, J. Ren, H. Feng, J. Yu, H. Liu, W. Chen, K. Wang and Y. Chen, *Small*, 2024, **20**, 2308473.
11. W. Liao, S. Zhou, Z. Wang, J. Long, M. Chen, Q. Zhou and Q. Wang, *J. Mater. Chem. A*, 2022, **10**, 21416-21421.